

Hardware-in-the-Loop Testing of Wide-Area Damping Controller for Field Implementation in Large-scale Power Grid

Xinlan Jia¹, Yi Zhao¹, Wenyong Yu¹, Yilu Liu^{1,2}

1. The University of Tennessee, Knoxville
2. Oak Ridge National Laboratory
TN, USA
xjia13@vols.utk.edu, {yzhao77, wyu10, liu}@utk.edu

Lin Zhu³, Evangelos Farantatos³,
Chengwen Zhang³
3. Electric Power Research Institute
(EPRI)
Palo Alto, CA, USA
{lzhu, efarantatos, czhang}@epri.com

Cosimo Pisani⁴, Giorgio Giannuzzi⁴,
Guido Coletta⁴, Salvatore Tessitore⁴
4. Terna,
Rome, Italy
{cosimo.pisani, giorgio.giannuzzi, guido.coletta, salvatore.tessitore}@terna.it

Abstract—In our previous work, an adaptive measurement-driven wide-area damping controller (WADC) for suppressing inter-area oscillations has been proposed and a hardware prototype was developed and validated through hardware-in-the-loop tests. As a continuation of the work, this paper introduces a WADC software prototype to handle the realistic challenges for field implementation in the control room of the power grid. The WADC software is developed and operated as an openPDC adapter with a graphical user interface (GUI) to monitor the WADC inputs and output, the communication delays and other variables. The software prototype has been fully tested through an enhanced hardware-in-the-loop (HIL) test setup. Its performance is verified under various realistic communication uncertainties, such as random time delays and data losses, with different communication protocols. The experiment results have proven the WADC software can deliver sufficient damping to suppress the targeted oscillation mode in handling various communication uncertainties for future field deployment.

Index Terms—wide-area damping controller (WADC), hardware-in-loop (HIL), inter-area oscillation, communication uncertainties

I. INTRODUCTION

In modern interconnected power grids, various types of oscillations have posed major threats to power system stability. Poorly damped inter-area oscillations are proven to have severe impacts on the secure operation of the interconnected power systems with the high penetration of Inverter-Based Resources (IBRs) and the retirement of synchronous generators [1], [2]. Phasor measurement units (PMUs) and wide-area measurement systems (WAMS) show advantages in the real-time monitor, detection and suppression of inter-area oscillations [3], [4]. By utilizing these remote synchronized measurements, wide-area damping controller (WADC) has been proven to be more effective on inter-area oscillations when comparing to the traditional local power system stabilizers [5], [6].

Several WADC design algorithms have been proposed based on system linearization with detailed models recently and demonstrated their efficiency through rigorous testing and simulations. Based on the linearized power grid model, a novel wide-area control strategy by modulating active power injection on the power system has been proposed in [6] to damp critical frequency oscillations. A novel static var compensator based WADC [7] with system linear model and particle swarm optimization (PSO) technique has been design and validated by simulation data. A robust WADC control technique [8], that is capable of damping forced oscillations and inter-area oscillations simultaneously, was designed and validated with various uncertainties and disturbances. However, accurate system models are difficult to be obtained due to the power grid complexity. In our previous studies, the effectiveness of an adaptive WADC control algorithm that employs measurement-driven system transfer functions without the knowledge of the detailed system model has been validated through a real oscillation event simulation [9]. Moreover, the proposed WADC technology has been validated to be able to adaptively update the controller parameters based on the corresponding operating condition in [10]. The WADC in [9] and [10] was implemented as a hardware prototype and tested with hardware-in-the-loop (HIL) setup in [11] and showed satisfactory performance. However, even though the proposed WADC algorithm has proven the effectiveness of the approach in damping oscillations based on simulation, it has not been implemented as a production level software for field demonstration in a realistic power grid. This paper serves as a follow-up to our previous work [9]–[11] and introduces a software prototype that was designed considering the realistic communication uncertainties for field implementation. The software prototype with a GUI is developed as an openPDC [12] adapter and is ready to be installed in the control room of the power grid for field demonstration.

The structure of this paper is organized as follows. In Section II, the structure of WADC software with GUI is demonstrated. Section III introduces the HIL test setup. The

This work was primarily supported by Electric Power Research Institute (EPRI), partly supported by National Science Foundation under the Award Number 1941101 and DOE Advanced Grid Modeling program. This work also made use of Engineering Research Center Shared Facilities supported by the Engineering Research Center Program of the National Science Foundation and DOE under NSF Award Number EEC-1041877 and the CURENT Industry Partnership Program.

test results that verify WADC damping performance under different communication uncertainties using both TCP/IP and UDP/IP communication protocol are presented in Section IV. Lastly, Section V summarizes the performance of the WADC software prototype and its potential developments in the future.

II. WADC SOFTWARE AND GUI IMPLEMENTATION AS OPENPDC ADAPTOR

The openPDC is an open-source Phasor Data Concentrator software tool designed to process time-series data streams in real-time. PMUs used as WADC inputs are configured to stream GPS-synchronized measurements to openPDC using IEEE C37.118 [13] communication protocol. This section will present how WADC software with a GUI is integrated into openPDC.

A. WADC software and its integration into openPDC

The WADC controller is integrated into openPDC as a user defined action, named WADC, which can collect PMU data from openPDC via its data interface. The structure of WADC in openPDC as well as the data flow is shown in Fig. 1. The software has two major components, one is the data adaptor module and the other one is the WADC control module.

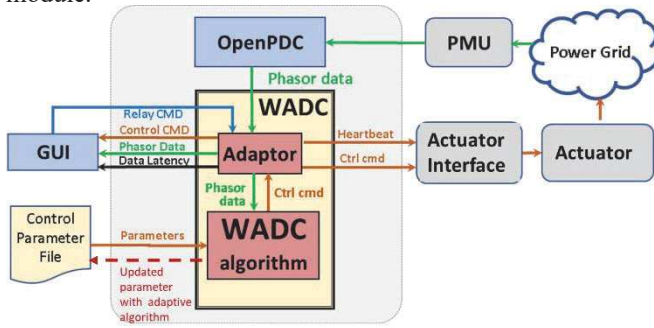


Figure 1. Diagram of openPDC, WADC and the data flow.

The data adaptor module is capable of converting the PMU measurement data from IEEE C37.118 format into the format required by the WADC algorithm. Once the openPDC is running as a Windows service, these modules will continually be forwarding the real-time PMU data from openPDC to WADC adaptor with the PMU reporting rate. In this paper, one primary PMU will be used as the WADC input under normal communication status. One backup PMU will be reserved when the primary PMU is unavailable. Both PMUs will continuously send real-time data using either UDP/IP or TCP/IP protocol to the WADC through the data adaptor. The data adaptor will also keep receiving the WADC output commands and sending these commands to user-defined destination IP addresses of the actuator communication interface using the IEEE C37.118 format with UDP/IP protocol. The command sending rate is controlled by an internal timer inside the WADC adaptor. Meanwhile, the adaptor will send the control command, phasor data and data latency to the GUI for displaying purpose. A heartbeat message with TCP/IP protocol will also be sent out from openPDC to the actuator communication interface to check the communication status from openPDC to the actuator.

B. Detailed WADC software function modules

The WADC control modules include both basic modules and advanced modules. The basic modules include washout, band-pass filters, lead-lag structure, command limiter and delay compensators that are implemented as transfer functions in [10]. The parameters of these transfer functions are initialized through a configuration file. These parameters in the configuration file are also able to be updated with real-time PMU measurements based on the proposed measurement-driven method. The advanced modules for handling real-world communication issues for field implementation include the following blocks:

1) *Delay Calculator*: The delays of both primary and backup PMU channels are calculated by comparing the timestamp of the PMU data with the local time of the server where openPDC is installed at the control room. The server is also time-synchronized with GPS by Network Time Protocol (NTP). These delays will be subsequently used for the data buffer module and supervisory control module.

2) *Data Buffer*: To avoid the frequent switching of the delay compensator parameters due to the random time delay, a data buffer with a threshold is designed to smooth the random delay impact. By comparing with the specified buffer threshold β_{buffer} , the data point whose delay is closest to the buffer threshold in the most recent 3 seconds PMU measurements is selected for the control command calculation per time step. Here the buffer threshold is set based on the statistical analysis of the communication delay between the PMU and the control center. β_{buffer} is selected to be the 98th percentile value of these calculated historical delays. This ensures that no less than 98% of the data can be accurately compensated.

3) *Negative Delay Detection*: The negative delay detection module is developed for WADC to detect the negative delay cases when the PMU channel or the server local time is not synchronized. A threshold for negative latency detection can be set as a parameter in openPDC. When the negative latency is over the threshold, WADC sends an alert message to the GUI, which will display this negative latency alert in its notification area with the delay value and its timestamp. Continuous negative delay exceeding -100ms in one PMU channel indicates the PMU channel has a large time synchronization error and cannot be used for WADC command calculation. In that case, WADC supervisory control module (described next) will be utilized to switch the WADC input PMU channel to the backup PMUs that have positive delays. If the negative latency detection keeps sending negative delay alarms for both the primary and backup PMUs, that indicates the time synchronization of the server is inaccurate and needs to be updated. In this case, the WADC is deactivated to prevent any unexpected adverse impact.

4) *Supervisory Control*: This module is developed to handle long-term data loss, communication outage and negative delays in real-world operation by switching between the primary and backup PMUs. This module determines the

PMU channel communication status by using the supervisory control positive threshold α_{pos} and negative threshold α_{neg} . If the delay of the selected data points from the data buffer module are always in the range $[\alpha_{neg} + \beta_{buffer}, \alpha_{pos} + \beta_{buffer}]$, the PMU channel is marked as good communication. Otherwise, it is marked as bad communication. There is a total of 6 supervisory control output: 0, 1, 2, 3, 4, and -1. The switch logic between each output status is shown in Fig. 2. All the supervisory control output and the corresponding PMU communication status and WADC status are listed in Table 1.

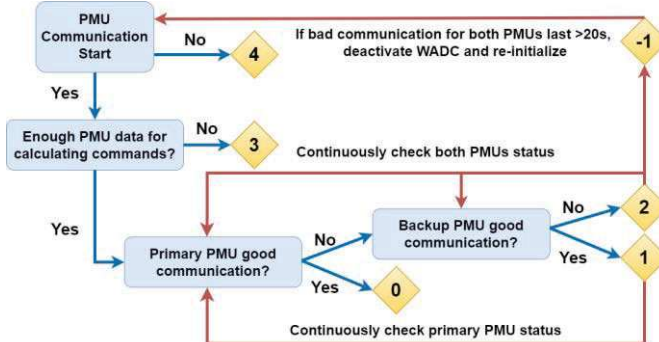


Figure 2. Flowchart of supervisory control module logic.

TABLE I. SUPERVISORY CONTROL OUTPUT AND WADC COMMUNICATION STATUS

Supervisor Control Output	WADC status	PMU communication status
-1	Re-initialization	Both primary and backup PMU communication are not recovered in 20s
0	Working with Primary PMU	Primary PMU: Normal
1	Working with backup PMU	Primary PMU: Measurement delay are out of $[\alpha_{neg} + \beta_{buffer}, \alpha_{pos} + \beta_{buffer}]$ Backup PMU: Normal
2	Deactivated	Both primary and backup PMUs' measurement delay are out of $[\alpha_{neg} + \beta_{buffer}, \alpha_{pos} + \beta_{buffer}]$
3	Deactivated	PMU communication established but haven't received enough datapoints ($>3s$) for control command calculation
4	Deactivated	PMU communication is not established

5) *Delay Calculator*: This module monitors the oscillation in the system and decides when to activate or deactivate the WADC control. If any of the frequency difference after the washout function is larger than the configured oscillation detector deadband, the oscillation detector will output 1. Otherwise, it will output 0. By multiplying the oscillation detector output to the control commands, the WADC actively sends control commands only when oscillations are detected.

The buffer threshold, supervisory control thresholds and oscillation detector deadband for the advanced modules are also configurable through the configuration file.

III. HARDWARE-IN-LOOP TESTING SETUP

To validate the performance of the developed WADC software under realistic field conditions, a HIL setup as shown

in Fig. 3 has been built at the University of Tennessee, which can emulate a large-scale power grid operating condition with measurement error/noise, random time delay, and different communication uncertainties. In this section, an introduction of the HIL setup with WADC for damping oscillations using the model of the continental Europe model will be given.

The Continental Europe Synchronous Area system with a detailed Italy power grid model is emulated on the OPAL-RT's real-time digital simulator OP5600 [14]. Two synchronous condensers at South Italy are used as the actuators of WADC to damp the North-South inter-area oscillation. The bus frequency PMU measurements are generated by the real-time simulator and collected by openPDC installed at a local computer. The local computer which represents the server at the control room synchronized its local clocks with GPS by NTP. The WADC adaptor at openPDC will generate the real-time control command based on the PMU measurements. The local executor is an enhanced PMU device that can receive the WADC control commands in a specified data frame and convert the digital control command into analog signal to modulate the condenser voltage reference. To test various communication network uncertainties between PMU, openPDC and the local executor in the laboratory environment, a communication network simulator, named KMAX [15], is included in the whole communication loop.

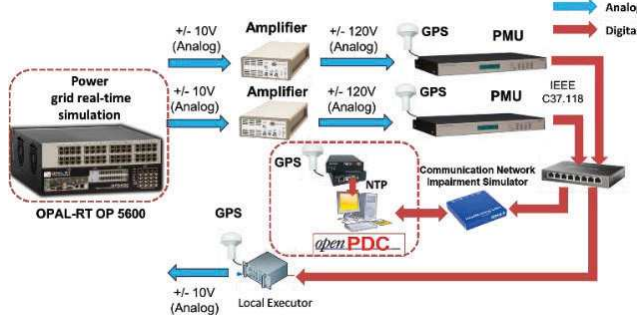


Figure 3. HIL test setup for WADC software prototype.

IV. DEMONSTRATING RESULTS

In this section, the WADC performance with different PMU communication protocols (TCP/IP and UDP/IP) under different communication uncertainties is discussed. The HIL test case is the replication of a North-South growing oscillation event that happened on December 3rd, 2017 in Continental Europe. In the HIL settings, the inherent communication delay is a constant around 600ms. Experiments that add various communication uncertainties on top of the inherent delay have been conducted in order to prove the delay compensation capability of the WADC software for future real-world field demonstration. The results on WADC constant delay tolerance, constant delay with random variation tolerance, random data drop tolerance, and supervisory control performance are presented in this section.

A. Oscillation damping performance under different constant time delay

The WADC damping performance is validated by the comparison between open-loop and closed-loop with different constant delays as shown in Fig. 4 and Fig. 5 for TCP/IP and UDP/IP. In the open-loop case, the oscillation is growing with negative damping ratio after the two events, respectively. After engaging the WADC with delay compensators, the damping ratio increased over 13% during the two events under both UDP/IP and TCP/IP protocols. The WADC significantly improved the inter-area oscillation damping and can tolerate up to 1000ms time delay.

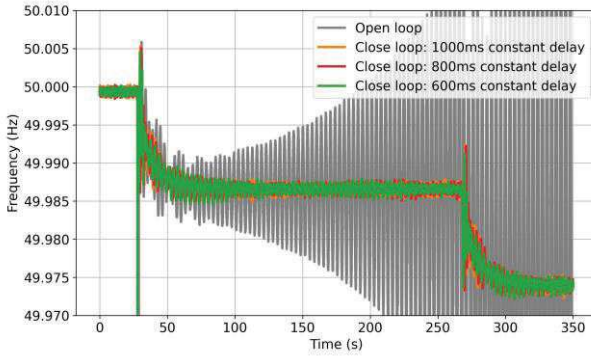


Figure 4. WADC oscillation damping performance with constant delay compensation under TCP/IP.

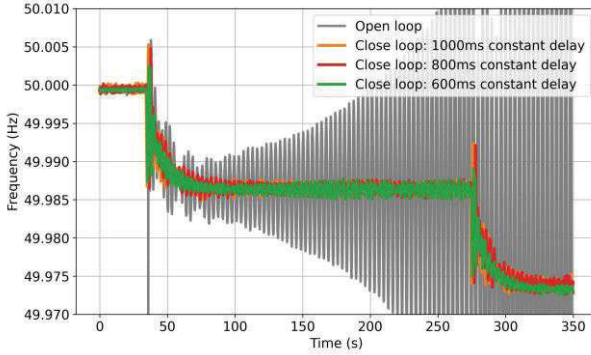


Figure 5. WADC oscillation damping performance with constant delay compensation under UDP/IP.

B. Random delay impact

In this experiment, constant delays with different magnitudes of random delay variations have been created to better mimic the actual power grid's largely varying time delays. 800ms and 1000ms constant delays with 50ms and 150ms random variations have been tested respectively. Fig.6 and Fig. 7 show that WADC can handle up to 1000ms constant delay with 150ms random variation for both communication protocols.

C. WADC random data drop tolerance

Different random data loss cases are simulated under both TCP and UDP protocols to check the WADC performance. As shown in Fig. 8 and Fig. 9, to guarantee the WADC performance, the random data drop tolerance for TCP/IP is around 5% while UDP can tolerate up to 90% random data drop. These results are caused by the communication

protocols' different data loss handling methods. For the PMU communication channel with a low data loss, both UDP/IP and TCP/IP can be used for WADC control.

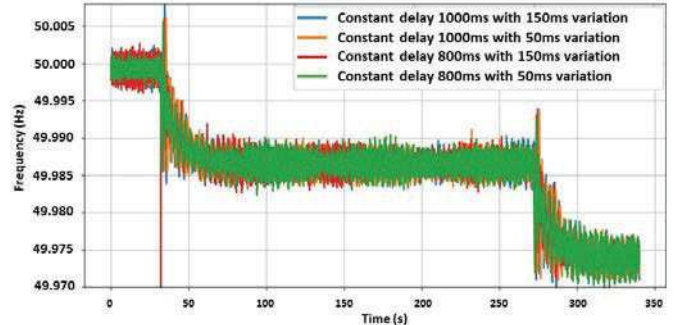


Figure 6. WADC performance for random delay compensation in TCP/IP.

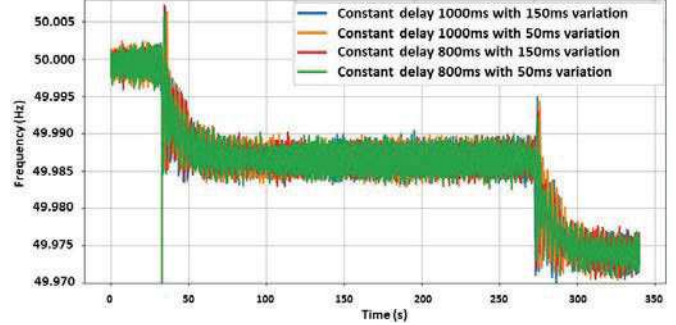


Figure 7. WADC performance for random delay compensation in UDP/IP.

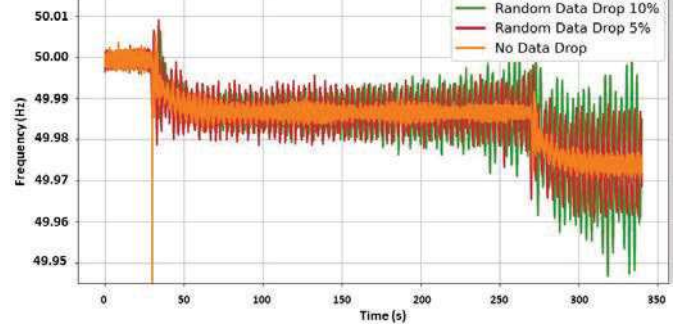


Figure 8. WADC random data drop tolerance for TCP/IP.

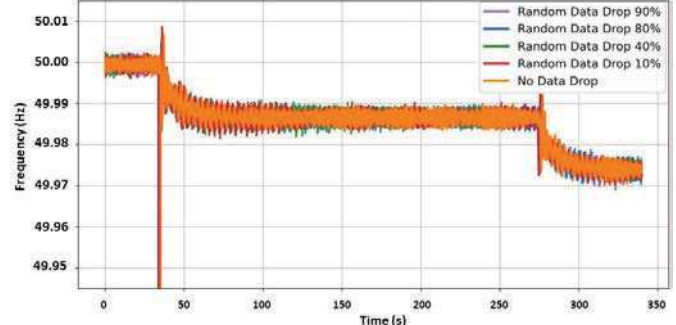


Figure 9. WADC random data drop tolerance for UDP/IP.

D. Chunk data loss with supervisory control performance

The chunk data loss and supervisory control functionality is tested by using the network simulator to introduce a 100s chunk data loss at primary PMU channel after the 1st generation disconnection event. The performance of WADC with and without supervisory control is compared for both protocols in Fig. 10 and Fig. 11. For TCP protocol, the system

becomes unstable without supervisory control due to the long recovery time of data (~ 150 s). On the contrary, the UDP protocol can have stable damping control performance due to the rapid data recovery time (~ 5 s).

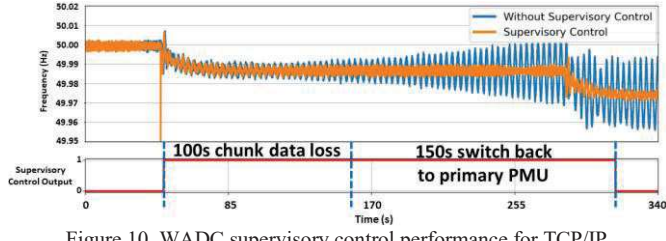


Figure 10. WADC supervisory control performance for TCP/IP.

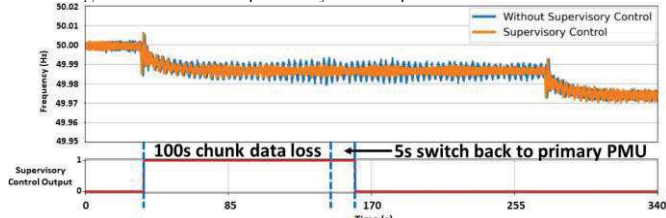


Figure 11. WADC supervisory control performance for UDP/IP.

E. Summary of HIL test results

The WADC software prototype's HIL tests performance is summarized in Table II. TCP and UDP protocols have similar damping performance when handling the constant and random delay compensation. However, due to the data recovery time difference between the two protocols for long-term data loss, the UDP/IP performs better for the tolerance of random data drop and chunk data loss.

TABLE II. HIL TEST SUMMARY

Protocol	Constant Delay Compensation	Random Delay Compensation	Random Data Drop	Chunk Data Loss with Supervisory Control
TCP/IP	Tolerate up to 1200ms constant delay	Tolerate up to 1000ms constant delay with 150ms random variation delay	Tolerate up to around 5% random data drop	Long waiting time for communication recovery (~ 150 s) after chunk data loss
UDP/IP	Tolerate up to 1200ms constant delay	Tolerate up to 1000ms constant delay with 150ms random variation delay	Tolerate up to 90% random data drop	Short recovery communication time (~ 5 s) after chunk data loss

V. CONCLUSION

In this paper, the WADC software prototype is developed as an openPDC adaptor along with a GUI to handle different communication uncertainties for field implementation. In order to validate the software prototype's control performance, HIL tests have been conducted for both TCP/IP and UDP/IP. During the HIL testing, a wide range of communication uncertainties have been simulated, including constant delay,

random delay, random data drop and chunk of data loss. These HIL testing results show that the WADC software can have effective damping performance under large constant and random delays for both communication protocols with the proper buffer size selection. However, UDP/IP would be recommended for the future field deployment of WADC with consideration of random data drop and chunk of data loss situations. The HIL experiments have provided valuable support for future field deployment of the wide-area damping controller in the Italy and any large-scale power grid.

REFERENCES

- [1] M. R. Younis and R. Iravani, "Wide-area damping control for inter-area oscillations: A comprehensive review," in *2013 IEEE Electrical Power & Energy Conference*, pp. 1-6.
- [2] G. Giannuzzi, V. Mostova, C. Pisani, S. Tessitore and A. Vaccaro, "Enabling Technologies for Enhancing Power System Stability in the Presence of Converter-Interfaced Generators," *Energies*, vol. 15, no. 21, p. 8064, Oct. 2022.
- [3] D. Lauria and C. Pisani, "A two-step procedure for on-line detection of power oscillations," *International Review of Electrical Engineering*, vol. 7, no. 4, pp. 4936-4937, 2012.
- [4] C. Olivieri et al., "Estimation of Modal Parameters for Inter-Area Oscillations Analysis by a Machine Learning Approach with Offline Training," *Energies*, vol. 13, no. 23, p. 6410, Dec. 2020.
- [5] V. Terzija, G. Valverde, D. Cai, P. Regulski, V. Madani, J. Fitch, S. Skok, M. M. Begovic and A. Phadke, "Wide-Area Monitoring, Protection, and Control of Future Electric Power Networks," *Proceedings of the IEEE*, vol. 99, no. 1, pp. 80-93, Jan. 2011.
- [6] R. Xie, I. Kamwa and C. Y. Chung, "A Novel Wide-Area Control Strategy for Damping of Critical Frequency Oscillations via Modulation of Active Power Injections," *IEEE Transactions on Power Systems*, vol. 36, no. 1, pp. 485-494, Jan. 2021.
- [7] K. Kumar, A. Prakash, P. Singh and S. K. Parida, "A Novel SVC Based Wide-Area Damping Controller for Inter-Area Oscillation," in *2021 IEEE 4th International Conference on Computing, Power and Communication Technologies (GUCON)*, pp. 1-6.
- [8] T. Surinkaw, R. Shah, S. M. Muyeen, N. Mithulanthan, K. Emami and I. Ngamroo, "Novel Control Design for Simultaneous Damping of Inter-Area and Forced Oscillation," *IEEE Transactions on Power Systems*, vol. 36, no. 1, pp. 451-463, Jan. 2021.
- [9] L. Zhu, Y. Zhao, Y. Liu, E. Farantatos, M. Patel, P. Dattaray, D. Ramasubramanian, L. Michi, E. Carlini, G. Giannuzzi and R. Zaottini, "Oscillation Damping Controller Design Using Ringdown Measurements for the Italian Power Grid," in *2019 IEEE Milan PowerTech*, pp. 1-6.
- [10] Y. Zhao, L. Zhu, H. Xiao, Y. Liu, E. Farantatos, M. Patel, A. Darvishi and B. Fardanesh, "An Adaptive Wide-Area Damping Controller via FACTS for the New York State Grid Using a Measurement-Driven Model," in *2019 IEEE Power & Energy Society General Meeting (PESGM)*, pp. 1-5.
- [11] C. Zhang, Y. Zhao, L. Zhu, Y. Liu, E. Farantatos, M. Patel, H. Hooshyar, C. Pisani, R. Zaottini and G. Giannuzzi, "Implementation and Hardware-In-the-Loop Testing of A Wide-Area Damping Controller Based on Measurement-Driven Models," in *2021 IEEE Power & Energy Society General Meeting (PESGM)*, pp. 1-5.
- [12] Github.com, "GridProtectionAlliance/openPDC", [online]. Available: <https://github.com/GridProtectionAlliance/openPDC>
- [13] IEEE Standard for Synchrophasor Measurements for Power Systems, IEEE Std C37.118.1-2011, Dec. 2011.
- [14] A. Semerow et al., "Dynamic Study Model for the interconnected power system of Continental Europe in different simulation tools," in *2015 IEEE Eindhoven PowerTech*, pp. 1-6.
- [15] The InterWorking Labs, "The KMAX Network Emulator", [online]. Available: <https://iwl.com/img/kmax-product-brief.pdf>